ISSN 2706-655X Vol. 7, Issue 3: 15-20, DOI: 10.25236/IJFET.2025.070303

# Photodetector Based on $Ag_2Se$ Quantum Dots

**Lipeng Wu**

*School of Physics and Opto-Electronic Engineering, Guangdong Provincial Key Laboratory of Sensing Physics and System Integration Applications, Guangdong University of Technology, Guangzhou, 510006, China*
*2112215036@mail2.gdut.edu.cn*

***Abstract:*** *With the emergence of new applications of infrared light detection technology, it is increasingly urgent to develop non-toxic and environmentally friendly alternative materials for heavy metal semiconductors. $Ag_2Se$ quantum dots (QDs) has a relatively narrow band gap and is highly suitable for optical detection in the near-infrared to mid-infrared spectral region. Moreover, $Ag_2Se$ QDs does not contain heavy metals and has a small impact on health and the environment. Due to the high electron mobility and wide spectral response characteristics of graphene and the high light absorption efficiency of QDs, the $Ag_2Se$ QDs/graphene composite photodetector (PDs) has the advantages of high response and wide spectral detection range. In this paper, we designed and constructed PDs based on $Ag_2Se$ QDs, and systematically studied the photoelectric detection performance. The photoelectric test of this device shows that under the irradiation of 808 nm light, Responsivity (R) is 342.24 A/W at a bias of 0.1 V, and Specific Detectivity (D*) is 3.35 × $10^{10}$ Jones. This work provides a reliable experimental idea for the preparation of high-performance infrared PDs.*

***Keywords:*** *Graphene, Photodetector, Quantum Dot*

## 1. Introduction

Near-infrared light detection technology has the advantages of long detection distance, good anti-interference performance and strong penetration ability of haze. Currently, near-infrared PDs is widely used in different fields, including biological imaging[1], explosive detection[2, 3], and space remote sensing[3]. Therefore, it is an urgent task to develop infrared and near-infrared PDs that are low-cost and easy to manufacture. Colloidal QDs have the advantages of low cost and easy mass production, and are an ideal choice for light-absorbing materials[4]. At present, the research on near-infrared PDs in the market mainly focuses on PbS QDs, whose detection rate is generally above $10^{13}$ Jones, comparable to that of commercial InGaAs PDs[5]. However, the use of lead-based and mercury-based QDs is not conducive to environmental protection. Encouragingly, $Ag_2Se$ QDs contains no heavy metals, is suitable for large-scale application, and has the least impact on health and the environment. Ayaskanta Sahu et al. reported for the first time that $Ag_2Se$ QDs achieved wavelength-tunable absorption in the near-mid-infrared range and could obtain tunable mid-infrared absorption under quantum constraints (>2.5 mm)[6].

$Ag_2Se$ belongs to one of the less explored types in the I-VI group compound semiconductor family. At room temperature, the bulk orthogonal $Ag_2Se$ has a direct narrow band gap of 0.15 eV. Due to its high carrier mobility and low thermal conductivity, it has attracted extensive attention as a promising thermoelectric material in recent years.

Graphene, as a two-dimensional material with unique physical, chemical and electrical properties, has received extensive attention in the field of ultrafast PDs in recent years. The excellent properties of graphene make it one of the ideal materials for manufacturing high-performance photodetectors. It can not only achieve a faster response speed for PDs, but also significantly improve its sensitivity and broaden the spectral response range, thereby meeting the demands of modern photoelectric detection technology for high performance and multi-functionality. Although graphene has many outstanding properties, its light absorption capacity is relatively weak, absorbing only about 2.3% of the incident light [7]. This property greatly limits the sensitivity of graphene PDs. To overcome this difficult problem, researchers are committed to exploring solutions that combine graphene with other semiconductor materials, leveraging the efficient light absorption characteristics of other semiconductors to enhance the overall performance[8].

The hybrid structure based on QDs and graphene has shown great application potential in the field of

ISSN 2706-655X Vol. 7, Issue 3: 15-20, DOI: 10.25236/IJFET.2025.070303

PDs. This hybrid structure has the following significant advantages: (1) The combination of graphene and QDs realizes the complementary advantages of the two materials. Graphene features high carrier mobility, excellent electrical conductivity and good thermal conductivity, while quantum dots have adjustable band gaps and efficient light absorption capabilities. When the two are combined, graphene can serve as an efficient charge transfer channel, rapidly transporting the carriers generated by quantum dots absorbing photons to the electrode, thereby significantly enhancing the efficiency of photocurrent generation. (2) Unlike traditional epitaxial growth techniques, the combination of graphene and QDs does not require strict lattice matching. In traditional semiconductor materials, lattice matching is a key factor in achieving high-quality heterostructures, but this requirement limits the range of material selection and increases the difficulty of preparation. As a single-atom-layer material, graphene has relatively independent atomic arrangement on its surface, and there is no lattice mismatch problem in the traditional sense between it and QDs. This enables researchers to flexibly select QDs of different sizes, compositions and bandgaps according to the requirements of specific applications, thereby optimizing the performance of PDs to meet different spectral responses and application requirements. (3) The ideal graphene surface has no dangling bonds, which ensures the formation of a high-quality interface between graphene and QDs, optimizing charge transfer and transport. The ongoing research and development of QDs/graphene hybrid PDs is expected to enhance the photosensing ability of graphene PDs.

In such studies, graphene mainly plays the role of a photogenerated carrier collection electrode or a charge transport channel. At present, this combination strategy has become a key research direction for the development of new graphene-based PDs.

## 2. Experiments

### *2.1 Materials*

Silver acetate (AgAc, Alfa-Aesar, 99.95%), selenium powder (Se, Acros, 99.95%), trioctylphosphine (TOP, Acros, 95%), oleamine (OAm, Acros, 80-90%), 1-octadecene (ODE, Aladdin, 90%), acetone (Sinopharm, 99.5%), hexane (Aladdin, >99%).

### *2.2 Preparation of Se precursors*

Weigh 188 mg of Se and carefully place it in 2 mL of TOP solution. Subsequently, ultrasonically treat the mixture and continue the ultrasonic operation until Se is completely dissolved in the TOP solution, forming a transparent and colorless uniform solution. After the dissolution is completed, the prepared Se precursor solution should be sealed and stored in a light-proof environment to ensure its stability and the smooth progress of subsequent reactions.

### *2.3 Synthesis of Ag2Se QDs*

Weigh 67 mg AgAc, 16 mL ODE and 4 mL OAm into a 100 mL three-necked flask, and mix the solution uniformly with ultrasonic waves to ensure that each component has full contact and is evenly dispersed. Subsequently, $N_2$ is introduced into the flask to prevent adverse reactions such as oxidation. Under the continuous stirring of the stirring device, the temperature inside the flask is gradually raised to 160℃. At this point, the mixture will gradually transform into a colorless and transparent clear solution,marking the completion of the second step of the operation. Take out the previously prepared 0.12 mL of Se precursor solution and quickly inject it into the reaction solution using a syringe. After injecting the Se precursor, the temperature of the reaction system was gradually reduced immediately to 140°C and maintained at this temperature for the reaction. The reaction time was set at 30 minutes. At this step, the Se precursor begins to undergo chemical reactions with other components in the reaction solution to generate the target product. After the reaction was completed, in order to separate the target product $Ag_2Se$ QDs, an appropriate amount of acetone was added to the reaction solution. The addition of acetone will cause the product to precipitate from the solution, forming a precipitate, thereby achieving the separation of the product from the reaction solvent.

Transfer the mixture containing the precipitate product to a centrifuge and perform centrifugation at a speed of 12000 rpm for 5 minutes. After centrifugation is completed, the precipitate is separated from the supernatant, and the obtained precipitate is the required $Ag_2Se$ QDs product. Finally, the product obtained by centrifugation is re-dispersed in the non-polar solvent hexane solution for subsequent storage or further processing.

ISSN 2706-655X Vol. 7, Issue 3: 15-20, DOI: 10.25236/IJFET.2025.070303

### *2.4 Fabrication of PDs*

Graphene films were deposited on $SiO_2$/Si wafers by mechanical exfoliation. This process can produce single or multi-layer graphene films. The electrode pattern was generated by UV maskless lithography and the Ti/Au (10 nm/100 nm) electrode was deposited by sputtering. $Ag_2Se$ QDs (~30 mg/mL) solution was spin-coated on the device, and $Ag_2Se$ QDs/graphene PDs were obtained after drying for 30 minutes.

### *2.5 Characterizations*

The absorption spectra were measured using a ultraviolet-visible spectrophotometer (GENESYS 150, Thermo Fisher Scientific). The morphology of quantum dots was studied by HT7700 transmission electron microscopy (TEM). The electrical characteristics at room temperature were analyzed using Keithley 4200 and SOFN 7SCF06A/B probe stations.

## 3. Results and discussion

$Ag_2Se$ is not a known traditional infrared semiconductor device material. When $Ag_2Se$ QDs grow to a diameter greater than 5.0 nm, QDs will become N-doped and thus enter the in-band $1S_e$-$1P_e$ optical transformation. The unique near-wave and mid-wave infrared physical properties brought about by the colloidal properties and in-band characteristics of QDs make $Ag_2Se$ QDs a technically interesting material platform for the development of infrared sensors.

High surface energy plays a crucial role in determining the total Gibbs free energy of the QD system, making it possible to obtain thermodynamically stable crystal structures, which are usually unstable in bulk. In the bulk, $Ag_2Se$ has a positively intersecting (β-$Ag_2Se$) structure and a very narrow band gap (0.15 eV). When $Ag_2Se$ is synthesized into nanoscale crystals with a size lower than 40 nm, they exhibit a crystal phase different from that of bulk.The $Ag_2Se$ QDs solution was dropped onto the copper mesh and left to dry. Then, its morphology was characterized using a transmission electron microscope. Through the high-resolution imaging of the transmission electron microscope, the morphology of $Ag_2Se$ QDs could be clearly seen. It can be observed from Figure 1 (a) that the distribution of $Ag_2Se$ QDs is relatively uniform, and there is no obvious aggregation phenomenon between the particles, showing good dispersibility. Through the statistical analysis of the size of a large number of particles, it was found that the average diameter of these $Ag_2Se$ QDs was 5.59 nm. The absorption spectra were measured by a ultraviolet-visible spectrophotometer (GENESYS 150, Thermo Fisher Scientific). As shown in Figure 2, the absorption peak of the $Ag_2Se$ QDs solution was at 652 nm.

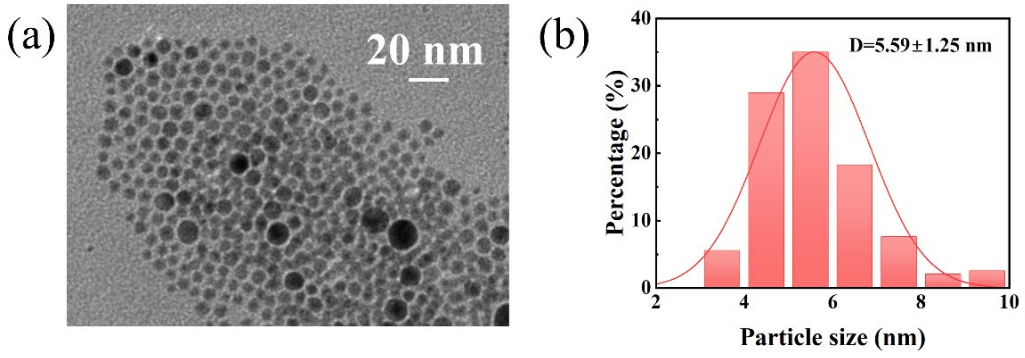


*Figure 1: (a) TEM image of $Ag_2Se$ QDs. (b) Particle size distribution of $Ag_2Se$ QDs.*

ISSN 2706-655X Vol. 7, Issue 3: 15-20, DOI: 10.25236/IJFET.2025.070303

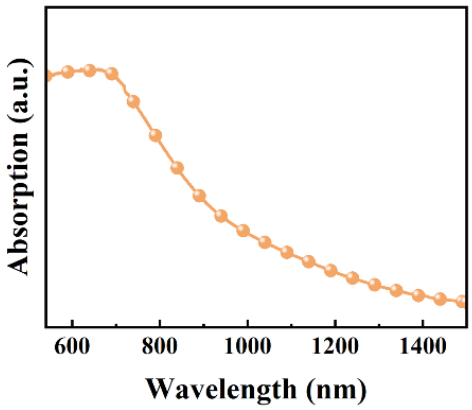


*Figure 2: Absorption Spectra of $Ag_2Se$ QDs.*

The working mechanism of PDs under light is divided into four stages. In the first stage, a negative peak was detected at the moment the light was turned on, as shown in Figure 3. This negative peak was composed of the current $I_{pyro}$ generated by the pyroelectric effect and the current $I_{photo}$ generated by the photoelectric effect. For pyroelectric materials with asymmetric structures, the change of temperature over time will induce pyroelectric polarization. When the light is turned on, the sharp rise in temperature triggers the pyroelectric effect. In addition, the temperature changes caused by infrared radiation generate thermal potential along the polar axis in pyroelectric materials. The generation and maintenance of thermoelectric potential can effectively regulate and control the charge transport in the junction region, and simultaneously regulate the photoelectric response process of local carriers. The pyroelectric current is positively correlated with the rate of temperature change (dT/dt). In the second stage, under continuous light conditions, the surface temperature of the quantum dots will gradually reach a steady state. Therefore, the temperature change rate dT/dt decreases to nearly zero, resulting in the disappearance of the pyroelectric current and the current returning to a stable photoelectric current. In the third stage, due to the sudden drop in temperature after turning off the lights, a sharp positive current ($-I_{pyro}$) is generated. In the fourth stage, the temperature returns to room temperature, and both the thermoelectric and photoelectric currents disappear, resulting in a current of zero. The pyroelectric effect is one of the key factors for improving the response speed. Compared with the photovoltaic effect, the photoelectric - thermoluminescence synergistic effect can significantly improve the response speed and specific detectivity rate of Pds.

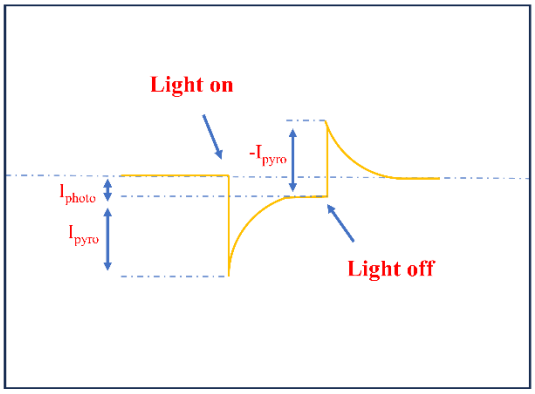


*Figure 3: The working principle of pyroelectric PDs.*

Here, we present the I-V curves of PDs under darkness and irradiation of different wavelengths, as shown in Figure 4. R is a key parameter in the performance evaluation of PDs, which directly reflects the detector's ability to convert incident light power into electrical signals. In other words, responsiveness measures how much photocurrent output a PDs can generate when it receives a certain amount of optical power. This parameter is crucial for evaluating the efficiency and sensitivity of a PDs. R is photocurrent density and the ratio of the incident light power, can be represented as $R = I_{ph}/PS = |I_{light}|-|I_{dark}|$, $I_{light}$ and $I_{dark}$ are photocurrent and dark current respectively, $I_{ph} = |I_{light}|-|I_{dark}|$ represents the total photocurrent

ISSN 2706-655X Vol. 7, Issue 3: 15-20, DOI: 10.25236/IJFET.2025.070303

amplitude (including pyroelectric current and photocurrent), P is the optical power density, and S is the effective photosensitive area. By testing the response rates under different wavelengths of light, it can be clearly seen that PDs has excellent optical response characteristics. At voltage of 0.1 V, the maximum optical response rate of PDs based on $Ag_2Se$ QDs is as high as 342.24 A/W (Figure 5 (a)). The response rate of the device can be further improved by applying a greater bias voltage. However, this device has material instability (due to the movement of silver ions), and applying a bias voltage higher than 0.5 V will cause irreversible degradation of the device.

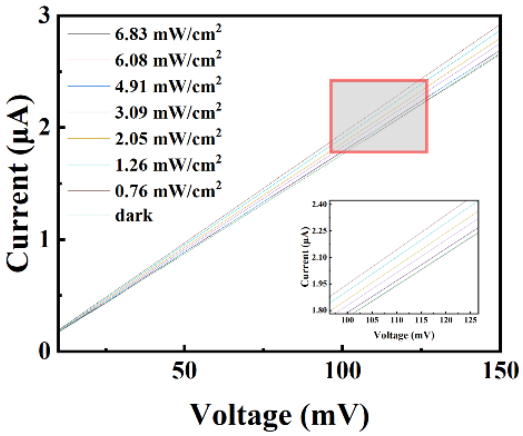


*Figure 4: I-V curves of $Ag_2Se$ QDs PDs at different optical power densities.*

D* is the core parameter for measuring the sensitivity of a device. It reflects the device's ability to detect weak optical signals under specific conditions and is the core indicator for measuring the sensitivity of PDs. It can be expressed by the formula: $D^* = R/\sqrt{2qI_{dark}S}$. Among them, q represents the charge of an electron. Here, we use the thermoelectric peak current to evaluate the gain of the device at different power densities. The maximum transient D* of PDs is as high as $3.35\times10^{10}$ Jones, indicating its excellent weak signal detection capability (Figure 5 (b)).

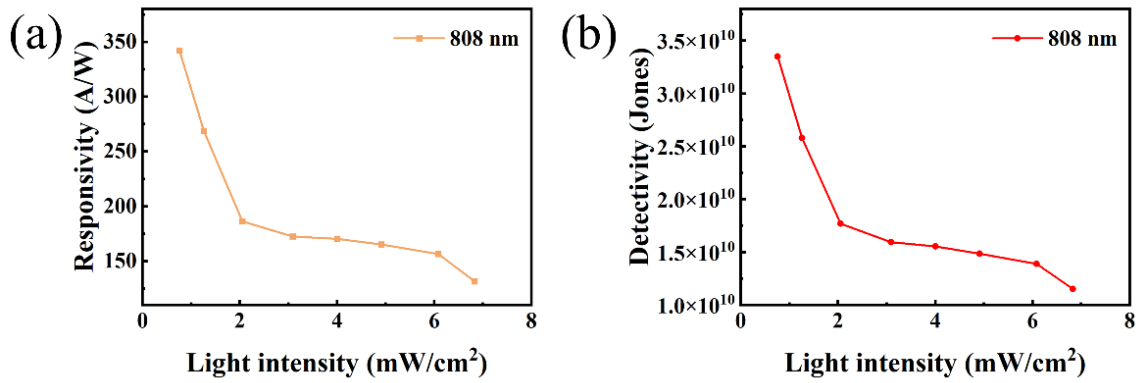


*Figure 5: (a) R and (b) D* of $Ag_2Se$ QDs PDs at 808 nm.*

The External Quantum Efficiency (EQE) of the device when the bias voltage is 0.1 V is shown in Figure 6. EQE represents the efficiency of PDs in converting photons of a certain wavelength into electrons and is related to the number of carriers that can be excited per photon. Use formula is expressed as: $EQE=I_{ph}hc/Pq\lambda=Rhc/q\lambda$, h is Planck's constant, c is the speed of light, λ is the wavelength of light. By optimizing material properties, device structure, surface treatment and working conditions, EQE can be effectively enhanced, thereby improving the performance and sensitivity of PDs. At zero bias voltage, without photoelectric gain, EQE cannot exceed 100%. However, under the bias voltage condition, due to the injection of charges into the photoconductor by the external circuit, a significant photoconductive gain is produced, which makes the EQE exceed 100%[9]. This gain mechanism is gradually suppressed at high light intensities for the following reasons: the space charge accumulation part shields the applied electric field[10], enhances non-radiative recombination (especially the Auge process) when the carrier density increases[11], and reduces the charge mobility due to thermal effects. These competitive effects jointly lead to the observed EQE decreasing with the increase of optical power density.

ISSN 2706-655X Vol. 7, Issue 3: 15-20, DOI: 10.25236/IJFET.2025.070303

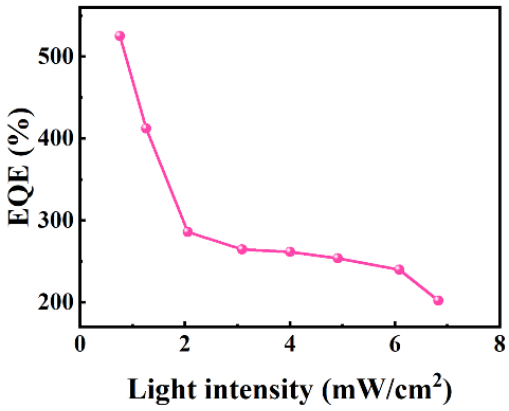


*Figure 6: EQE of $Ag_2Se$ QDs PDs.*

## 4. Conclusions

To fill the gap in the application of $Ag_2Se$ QDs in the field of photoelectric detection, we constructed a hybrid PDs based on $Ag_2Se$ QDs/graphene. Under a bias voltage of 0.1 V, the R of this PDs can reach 342.24 A/W and the D* is $3.35 \times 10^{10}$ Jones. This PDs has achieved an excellent photoelectric detection performance. We will continue to optimize the material parameters and further enhance the performance to provide support for the development of PDs.

## References

*[1] Wu Z, Zhai Y, Kim H, et al. Emerging Design and Characterization Guidelines for Polymer-Based Infrared Photodetectors [J]. Acc Chem Res, 2018, 51(12): 3144-3153.*
*[2] Gundepudi K, Neelamraju P M, Sangaraju S, et al. A review on the role of nanotechnology in the development of near-infrared photodetectors: materials, performance metrics, and potential applications [J]. Journal of Materials Science, 2023, 58(35): 13889-13924.*
*[3] Martyniuk P, Antoszewski J, Martyniuk M, et al. New concepts in infrared photodetector designs [J]. Appl Phys Rev, 2014, 1(4).*
*[4] Xu W, Liu J, Dong B, et al. Atomic-scale imaging of ytterbium ions in lead halide perovskites [J]. Sci Adv, 2023, 9(35): eadi7931.*
*[5] Bothra U, Albaladejo-Siguan M, Vaynzof Y, et al. Impact of Ligands on the Performance of PbS Quantum Dot Visible–Near-Infrared Photodetectors [J]. Adv Opt Mater, 2022, 11(1): 2201897.*
*[6] Sahu A, Khare A, Deng D D, et al. Quantum confinement in silver selenide semiconductor nanocrystals [J]. Chem Commun, 2012, 48(44): 5458-5460.*
*[7] Nair R R, Blake P, Grigorenko A N, et al. Fine Structure Constant Defines Visual Transparency of Graphene [J]. Science, 2008, 320(5881): 1308-1308.*
*[8] Chen Z, Cheng Z, Wang J, et al. High Responsivity, Broadband, and Fast Graphene/Silicon Photodetector in Photoconductor Mode [J]. Adv Opt Mater, 2015, 3(9): 1207-1214.*
*[9] Lee J W, Kim D Y, So F. Unraveling the Gain Mechanism in High Performance Solution-Processed PbS Infrared PIN Photodiodes [J]. Adv Funct Mater, 2015, 25(8): 1233-1238.*
*[10] Ahmadi R, Abnavi A, Ghanbari H, et al. Self-powered, broadband, and polarization-sensitive pyroelectric-photoelectric photodetector based on silicon-water heterojunction [J]. Nano Energy, 2022, 98: 107285.*
*[11] Kolli C S R, Selamneni V, B A M M, et al. Broadband, Ultra-High-Responsive Monolayer $MoS_2/SnS_2$ Quantum-Dot-Based Mixed-Dimensional Photodetector [J]. ACS Appl Mater Interfaces, 2022, 14(13): 15415-15425.*